

## Dynamics of Vortices in Underdamped Josephson-Junction Arrays

H. S. J. van der Zant, F. C. Fritschy, T. P. Orlando,<sup>(a)</sup> and J. E. Mooij

*Department of Applied Physics, Delft University of Technology,*

*P.O. Box 5046, 2600 GA Delft, The Netherlands*

(Received 5 November 1990)

Vortex motion has been studied for the first time in high-quality, highly underdamped, two-dimensional Josephson-junction arrays, with normal-state junction resistances ranging from 43  $\Omega$  to 48 k $\Omega$ . Strong similarity is found with the dynamics of the phase in single junctions, e.g., vortices with mass moving in the spatially periodic washboard potential of the 2D array. High-resistance arrays show resistance below 35 mK due to either thermally activated depinning or quantum fluctuations.

PACS numbers: 74.50.+r, 74.60.Ge, 74.60.Jg

Fabricated two-dimensional Josephson-junction arrays are model systems for the study of vortex motion in 2D superconductors, where parameters are well known and can be varied over orders of magnitude. So far, experimental studies of arrays have been concentrated on overdamped junctions and viscous vortex flow. Vortex dynamics in systems with low dissipation is very interesting from a theoretical point of view, and its understanding may be very relevant for the interpretation of experimental data on high-resistance superconducting films. Theoretical predictions have been made for the quantum behavior of vortices,<sup>1-4</sup> ballistic motion,<sup>3,5</sup> and Aharonov-Casher oscillations of quantum vortices moving in a ring around charge.<sup>6</sup> Superconductor-insulator transitions occur as a function of the ratio of charging energy versus Josephson coupling energy,<sup>7,8</sup> and as a function of magnetic field.<sup>9</sup> Vortex dynamics near those transitions are of special interest. In this paper we present the first experimental data on vortices in arrays of high-quality strongly underdamped aluminum tunnel junctions, which we see as the necessary first steps towards studies of the fascinating predicted effects. We find that the whole picture of vortex motion in the array is closely analogous to the dynamics of the phase in single underdamped Josephson junctions.

In underdamped arrays, the junction capacitance leads to a mass term in the equation of motion. A vortex moving with velocity  $u$  produces a voltage across a junction  $V = (\Phi_0/2\pi)\dot{\phi}$ , where  $\Phi_0$  is the flux quantum and  $\phi$  is the phase difference with a time rate of change proportional to  $u$ . The sum of the charging energies  $\frac{1}{2}CV^2$ , where  $C$  is the junction capacitance, can be viewed as a kinetic-energy term. It is proportional to  $u^2$ , which defines the effective vortex mass  $M_v$ . In a quasistatic approach,<sup>2-5</sup> one finds<sup>10</sup>  $M_v = (\Phi_0/2\pi)^2 C/2$ . In this form,  $M_v$  is connected with the velocity normalized to  $p/2\pi$ , with  $p$  the lattice constant. In junction arrays vortices move in a two-dimensional periodic potential with energy minima in the center of each unit cell. To move from one cell to the next in a square array, the vortex has to overcome an energy barrier<sup>11</sup>  $U_{\text{bar}} = 0.2E_J(T)$ , where  $E_J(T)$  is the

Josephson coupling energy,  $E_J(T) = \Phi_0 i_{c0}(T)/2\pi$  with  $i_{c0}$  the intrinsic junction critical current. The equation of motion for a single vortex moving along a row of cells in an infinite square array can be written as<sup>4</sup>

$$M_v \ddot{x} + \eta \dot{x} = E_J(T) \{0.1 \sin x + i/i_{c0}\}. \quad (1)$$

Here,  $x$  is the position normalized by  $p/2\pi$ ,  $i$  the applied transport junction current in the direction perpendicular to  $x$ , and  $\eta$  the viscosity given<sup>4,5</sup> by  $\eta = (\Phi_0/2\pi)^2/2r_e$ , with  $r_e$  the effective damping resistance. In Eq. (1), the periodic array potential is modeled with a cosine function, which is a good approximation.<sup>12</sup> There is a direct analogy between the motion of a vortex in an array and the dynamics of a single Josephson junction. Equation (1) also holds for the time dependence of  $\phi$  in the resistively and capacitively shunted junction model for a junction with critical current  $0.1i_{c0}$ , a capacitance  $C/2$ , and a shunt resistance  $2r_e$ . In analogy with single junctions, we define a McCumber parameter for vortices  $\beta_{c,v} = 0.4\pi i_{c0} r_e^2 C/\Phi_0$  and a plasma frequency  $\omega_{p,v} = (0.4\pi i_{c0}/\Phi_0 C)^{1/2}$ .

Samples contain high-quality all-aluminum Josephson tunnel junctions made with a shadow-evaporation technique. Different junction normal-state resistances  $r_n$  are obtained by varying the oxidation pressure. Junctions are arranged in a square network. Arrays have a length  $L$  of 300 unit cells and a width  $W$  of 100 unit cells, or have  $L=200$  and  $W=40$ . The intrinsic array critical current  $I_{c0}(T)$  is  $I_{c0}(T) = (W+1)i_{c0}(T)$ , where  $i_{c0}(T)$  is given by the Ambegaokar-Baratoff value with a critical temperature  $T_c = 1.25$  K. At  $T=0$ ,  $i_{c0}r_n = 300 \mu\text{V}$ . The area of the elementary cell  $p^2 = 49 \mu\text{m}^2$  and the junction area is about 0.7 or 1.4  $\mu\text{m}^2$ . The Josephson coupling energy is dominant over the charging energy  $E_c = e^2/2C$ .

Experiments are performed in a dilution refrigerator inside Mumetal and lead magnetic shields. Small perpendicular magnetic fields can be applied by two coils of superconducting wire, placed in a Helmholtz configuration. The applied field is given as the frustration  $f$ , the flux per unit cell divided by  $\Phi_0$ . Electrical signals

from low-resistance samples ( $r_n < 1$  k $\Omega$ ) are filtered only at room temperature, whereas for high- $r_n$  samples additional filtering is applied in the mixing chamber in the low-temperature environment. An independent estimate of the capacitance of the  $0.7\text{-}\mu\text{m}^2$  junctions is obtained from the Coulomb gap of high-resistance samples, measured in a magnetic field of 2 T at a temperature of 10 mK. We find  $C \approx 80$  fF. We assume  $C \approx 160$  fF for the  $1.4\text{-}\mu\text{m}^2$  junctions. At  $T=0$ , the effective flux penetration depth varies from  $5p$  for samples with  $r_n = 43$   $\Omega$  to  $2500p$  for samples with  $r_n = 20$  k $\Omega$ .

In zero magnetic field, we only observe hysteretic step-like increases of the voltage.<sup>13</sup> At each step the voltage jumps by the gap value of  $2\Delta/e$  ( $=382$   $\mu\text{V}$ ) or multiples of that value. Related behavior was seen in 2D arrays of niobium tunnel junctions.<sup>14</sup> Each step corresponds to localized collective switching into the dissipative state of one cross row of junctions. In the following, we denote this process of steplike increases as single-row switching. In nonzero magnetic fields, we do observe flux-flow behavior in a limited current-voltage window. There is a depinning current ( $I_{\text{dep}}$ ) which for low-resistance samples ( $r_n < 110$   $\Omega$ ) is nearly equal to the value of  $0.1I_{c0}$  as predicted from Eq. (1). High-resistance samples have  $I_{\text{dep}} < 0.1I_{c0}$ . For high voltages, single-row switching occurs, initiated by vortices which move with their maximum velocity. In long Josephson junctions, the maximum vortex velocity is determined by the phase velocity of propagating electromagnetic waves. Similar behavior is expected in 2D arrays.<sup>15</sup> For  $f < 0.15$ , the maximum velocity in our low-resistance samples is in good agreement with the calculations of Ref. 15; for high-resistance samples the switching occurs at much lower voltages than predicted. More details on this will be published in a subsequent paper. Further, there is an entry field for vortices. When  $W=100$ , for  $f < 0.02$  we only observe single-row switching. In previous measurements,<sup>16</sup> we found that for an array with  $W=63$  the energy barriers at the edge disappear at  $f \approx 0.02$ .

We have performed measurements on eight different arrays, with  $r_n$  ranging from 43  $\Omega$  to 48 k $\Omega$ . We concentrate on the flux-flow behavior at low temperatures ( $T < 700$  mK) and small magnetic fields ( $f < 0.2$ ). We first discuss the results for low-resistance samples with  $r_n < 200$   $\Omega$  and show in particular the measurements for sample A which has  $r_n = 80$   $\Omega$  and  $C = 160$  fF. In Fig. 1, current-voltage  $I$ - $V$  characteristics are given, measured for  $f=0.1$  at  $T=640$  and 10 mK. At these temperatures,  $I_{c0}$  is 335 and 379  $\mu\text{A}$ .

At  $T=640$  mK, the voltage is zero within measuring accuracy for  $I < 32$   $\mu\text{A}$ . For  $V > 150$   $\mu\text{V}$  the voltage is almost linear in  $I$ . We call this the flux-flow regime. The extrapolation of the  $I$ - $V$  curve in this regime intersects the  $V=0$  axis at about 40  $\mu\text{A}$ . We choose the depinning current  $I_{\text{dep}}$  as the current for which  $V=2$   $\mu\text{V}$ . For sample A at 640 mK, we find  $I_{\text{dep}} = 33$   $\mu\text{A}$ , which is

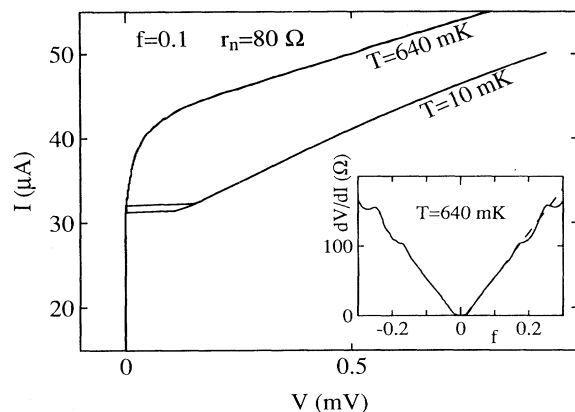


FIG. 1. Current-voltage characteristic of sample A, measured in a magnetic field of  $f=0.1$  at a temperature of 640 mK (upper curve) and at  $T=10$  mK (lower curve). Inset: The dynamic resistance  $dV/dI$  vs frustration. The dynamic resistance has been measured with a lock-in technique,  $I_{\text{bias}}=60$   $\mu\text{A}$ ,  $I_{\text{osc}}=1$   $\mu\text{A}$ .

$0.1I_{c0}$  as expected from Eq. (1). The depinning current is almost constant in the range  $0.1 < f < 0.2$ . We have measured the slope of the  $I$ - $V$  characteristic ( $dV/dI$ ) in the flux-flow regime as a function of  $f$ . For  $T=640$  mK the result is shown in the inset of Fig. 1. For  $0.03 < f < 0.2$  the resistance is linear in  $f$ . Flux-flow resistance in junction arrays has been calculated<sup>5</sup> in a Bardeen-Stephen-like treatment, giving  $R_{\text{ff}} = (L/W) \times f2r_e$ . From the inset in Fig. 1, we find  $r_e = 1.3r_n$ .

For the curve measured at 10 mK the voltage switches to a finite value and becomes hysteretic. This hysteresis is found for temperatures  $T < 0.5$  K and is very different from the hysteresis associated with single-row switching to the gap voltage, which appears at much higher voltages and currents. The current where the array jumps to the  $V \neq 0$  state is  $0.085I_{c0}$ . The dynamic resistance is again linear in  $f$  for  $0.03 < f < 0.2$ . From the slope of the  $r(f)$  plot we find that  $r_e = 1.2r_n$ . For this array,  $\beta_{c,v} = 2.3$  when  $r_e$  is taken to be  $r_n$ . We did not find hysteresis at low voltages for an array with  $r_n = 43$   $\Omega$ , whereas clear hysteresis was observed for another array with  $r_n = 80$   $\Omega$  and an array with  $r_n = 110$   $\Omega$ . The junction capacitance is 160 fF for these arrays and  $\beta_{c,v}(r_n)$  is 1.3, 2.3, and 3.2, respectively. At  $f=0.15$  and  $T=10$  mK, the ratio  $I_{\text{dep}}/I_{c0}$  is 0.10 for the 43- $\Omega$  sample, 0.105 for the 80- $\Omega$  sample, and 0.09 for the 110- $\Omega$  sample. When in the flux-flow regime the dynamic resistance of these arrays is measured as a function of  $f$ , it increases again linearly with  $f$  for small  $f$  and we find values of  $r_e$  close to  $r_n$ .

Summarizing our experimental results on the low-resistance samples, we find that there are striking similarities with single underdamped shunted junctions. For values of  $\beta_{c,v}$  above 1 we observe hysteresis in the  $I$ - $V$

characteristic. The hysteresis is due to the inertial mass of vortices, which escape out of the wells of the periodic lattice potential. We observe flux-flow behavior above a depinning current close to the intrinsic value of  $0.1I_{c0}$ . The shape of the  $I$ - $V$  characteristic does not fully correspond to the result for a single shunted Josephson junction. It rather resembles the  $I$ - $V$  of a single superconducting microbridge. We see an offset of the asymptote in the positive current direction ("excess current"). This may indicate that treating the vortex as a more or less rigid object in a sinusoidal potential is an oversimplification. Flux-flow measurements indicate that the effective damping resistance is of the order of  $r_n$ . This may be due to the fact that the plasma frequency of the single junctions is close to the gap frequency.

We now consider the measurements on the high-resistance samples. We discuss data of sample B, which has  $r_n = 20.6$  k $\Omega$  and  $C = 160$  fF. At 10 mK,  $I_{c0}$  is 1.47  $\mu$ A. A typical example of a low-temperature  $I$ - $V$  characteristic is shown in Fig. 2. The curve is taken at  $f = 0.15$ . For all three samples which have  $r_n > 10$  k $\Omega$ , a finite resistance is observed around zero current in a magnetic field. For sample B, this zero-bias resistance is 33  $\Omega$ . In Fig. 2 at about 5 nA, the resistance starts to increase. For high currents  $dV/dI$  is 2 k $\Omega$ . We find that  $I_{\text{dep}} = 7$  nA, and  $I_{\text{dep}}/I_{c0} = 0.005$ . In the inset of Fig. 2, we have plotted  $I_{\text{dep}}/I_{c0}$ , obtained from  $I$ - $V$  characteristics at  $f = 0.15$  and  $T = 10$  mK, as a function of  $r_n$ . Clearly, a systematic decrease of this ratio is found with increasing  $r_n$ . We have measured the zero-bias resis-

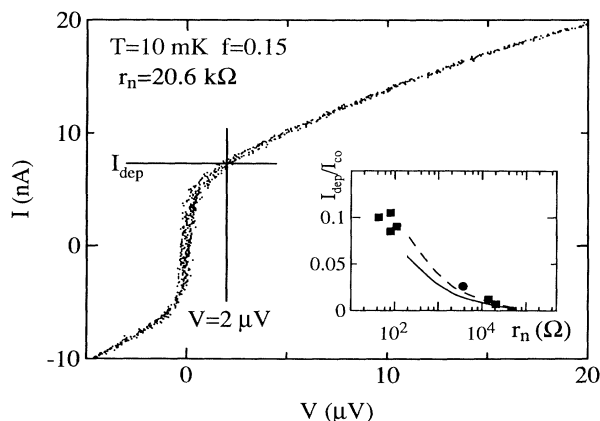


FIG. 2. Current-voltage characteristic of sample B, measured at  $f = 0.15$  and  $T = 10$  mK, showing the definition of the depinning current with the 2- $\mu$ V criterion. Inset: The ratio of the array depinning current to the array critical current as a function of the junction normal-state resistance. The depinning current is obtained from  $I$ - $V$  curves measured at  $f = 0.15$  and  $T = 10$  mK. The circles give the results for samples, which have  $C = 80$  fF, and the squares the ones for the other samples with  $C = 160$  fF. The dashed and solid line present retrapping currents calculated in analogy with single-junction McCumber theory for  $C = 80$  and 160 fF, respectively.

tance and  $dV/dI$  at 14 nA with a lock-in technique as a function of  $T$ . At  $T = 400$  mK, the two resistances are equal. With decreasing temperature, the zero-bias resistance decreases exponentially, but at 35 mK the resistance levels off at the value of 33  $\Omega$ . In contrast, the dynamic resistance at 14 nA, is almost temperature independent up to 400 nK. As a function of  $f$ , the resistance at 14 nA increases linearly with  $f$  for  $0.03 < f < 0.2$ . From the  $R(f)$  slope, we find  $r_e = 0.1r_n$ .

At low temperatures and for small fields (independent vortex motion), the array resistance can be written as  $R \approx L\Phi_0 f / i\langle\Delta t\rangle$ , where  $\langle\Delta t\rangle$  is the average time for crossing the whole array. At low current levels, pinning is dominant and  $\langle\Delta t\rangle$  is limited by the escape time out of the periodic potential. The escape can be due to thermal activation (TA) over the barrier or to macroscopic quantum tunneling (MQT). After one escape, a vortex can be retrapped in the next well. In this vortex-creep regime  $\langle\Delta t\rangle \approx W/\Gamma$ , where  $\Gamma$  is the net rate for escape out of a well. Using the analogy with single junctions, we have calculated the escape rates for TA and MQT in the moderate to strongly underdamped limit.<sup>17</sup> TA can explain the zero-bias resistance of sample B, if we assume  $r_e$  in the order of  $r_n$ . To explain the leveling off below 35 mK an effective noise temperature of 35 mK has to be assumed. However, in our high-resistance arrays the vortex plasma frequency is at least 1 order of magnitude smaller than the gap frequency of the single junctions. Therefore, one could argue that  $r_e$  should be determined by the subgap resistance. If we take  $r_e = 1000r_n$  no reasonable fit can be made. For  $r_e = r_n$ , MQT predicts a zero-bias resistance at  $T = 10$  mK, which is a factor 4 larger than the experimentally observed value. With  $r_e = 1000r_n$ , the MQT prediction is different by a factor 7. Considering the uncertainties in  $M_n$  and  $C$ , which appear in the exponent of the MQT rate, we cannot exclude the possibility of vortex MQT. In the absence of quantitative theoretical predictions, we cannot distinguish between TA and MQT, although it seems more likely that we are dealing with TA as the barrier height corresponds to a temperature of 70 mK.

At higher currents, the periodic potential is tilted so far that after escaping, vortices keep moving over the next and subsequent barriers (running state). Again we have to distinguish between TA and MQT. In the case of TA the resistance increases sharply when the vortex is no longer retrapped in the next well. In the  $I$ - $V$  characteristic the transition from low-creep resistance to high flux-flow resistance at this retrapping current looks very similar to depinning at the critical current but has a very different physical background. Also in single junctions, the role of the retrapping current as the apparent critical current has been observed.<sup>18</sup> For vortices, we calculate  $I_{\text{dep}}$  as the retrapping current in analogy with single-junction McCumber theory. Taking  $r_e = r_n$ , the calculated values are close to the measured ones (inset in Fig. 2).

When vortices escape by MQT without energy loss, the “depinning” current can be estimated as the current which has tilted the periodic potential so far that the ground level of the oscillation in the well  $E_0 = \frac{1}{2} \hbar \omega_{p,v}$  lies at the same energy as the next barrier ( $3\Phi_0 i/2 = 0.2E_J - E_0$ ). For high-resistance arrays, the calculated values lie within a factor of 2 of the measured ones.

The flux-flow resistance, determined to be around 14 nA for sample 7, is almost independent of temperature up to 400 mK. The value is remarkably low, around  $0.1r_n$ . As the barrier energy  $0.2E_J$  is about 70 mK, the escape probability above 150 mK is very close to 1. So apparently vortices experience damping stronger than that corresponding to  $r_n$ . This observation seems to indicate that vortices can lose energy in a way different from Ohmic dissipation. Probably, energy is left in functions oscillating at their plasma frequency in the wake of the vortex.

In conclusion, we have reported on vortex motion in semiclassical underdamped Josephson-junction arrays. We have found that new and interesting phenomena occur which demonstrate, for the first time, the importance of the vortex mass in determining the dynamics of vortices. We have observed vortex creep, retrapping, as well as a running state of vortices and possible quantum fluctuations in the position of the vortex.

We thank P. Hadley, L. J. Geerligs, K. K. Likharev, G. Schön, P. A. Bobbert, U. Eckern, and A. Schmid for very valuable discussions. Samples were made at the Delft Institute for Submicron Technology (DIMES). Part of the work was supported by the Dutch Foundation for Fundamental Research on Matter (FOM). T.P.O. acknowledges the support of the National Science Foundation through Grant No. DMR-8802613.

<sup>(a)</sup>Permanent address: Department of Electrical Engineer-

ing and Computer Science, Massachusetts Institute of Technology, Cambridge, MA 02139.

<sup>1</sup>E. Simanek, Solid State Commun. **48**, 1023 (1983).

<sup>2</sup>S. E. Korshunov, Physica (Amsterdam) **152B**, 261 (1988); A. I. Larkin, Yu. N. Ovchinnikov, and A. Schmid, *ibid.* **152B**, 266 (1988).

<sup>3</sup>U. Eckern and A. Schmid, Phys. Rev. B **39**, 6441 (1989).

<sup>4</sup>U. Eckern, in “Applications of Statistical and Field Theory Methods to Condensed Matter,” Proceedings of the NATO Advanced Study Institute, Evora, Portugal, May 1989 (to be published).

<sup>5</sup>T. P. Orlando, J. E. Mooij, and H. S. J. van der Zant, Phys. Rev. B (to be published).

<sup>6</sup>B. J. van Wees, Phys. Rev. Lett. **65**, 255 (1990).

<sup>7</sup>A number of articles can be found in Physica (Amsterdam) **152B**, 1–302 (1988).

<sup>8</sup>L. J. Geerligs, M. Peters, L. E. M. de Groot, A. Verbruggen, and J. E. Mooij, Phys. Rev. Lett. **63**, 326 (1989).

<sup>9</sup>M. P. Fisher, Phys. Rev. Lett. **65** 923 (1990); A. F. Hebard and M. A. Paalanen, Phys. Rev. Lett. **65**, 927 (1990).

<sup>10</sup>In general, the vortex mass contains a quasiparticle term as well as a contribution from the geometrical capacitance (see, e.g., Ref. 3). We ignore the first.

<sup>11</sup>C. J. Lobb, D. W. Abraham, and M. Tinkham, Phys. Rev. B **27**, 150 (1983).

<sup>12</sup>M. S. Rschowski, S. P. Benz, M. Tinkham, and C. J. Lobb, Phys. Rev. B **42**, 2041 (1990).

<sup>13</sup>H. S. J. van der Zant, F. C. Fritschy, T. P. Orlando, and J. E. Mooij, Physica (Amsterdam) **165 & 166B**, 969 (1990).

<sup>14</sup>H. S. J. van der Zant, C. J. Muller, L. J. Geerligs, C. J. P. M. Harmans, and J. E. Mooij, Phys. Rev. B **38**, 5154 (1988).

<sup>15</sup>K. Nakajima and Y. Sawada, J. Appl. Phys. **52**, 5732 (1981).

<sup>16</sup>H. S. J. van der Zant, H. A. Rijken, and J. E. Mooij, J. Low Temp. Phys. **79**, 289 (1990).

<sup>17</sup>H. Grabert, P. Olschowski, and U. Weiss, Phys. Rev. B **36**, 1931 (1987).

<sup>18</sup>M. Iansiti, A. T. Johnson, W. F. Smith, H. Rogalla, C. J. Lobb, and M. Tinkham, Phys. Rev. Lett. **59**, 489 (1987).